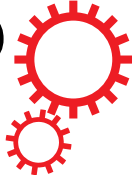


SCIENTIFIC REPORTS



OPEN

The Quantum Biology of Reactive Oxygen Species Partitioning Impacts Cellular Bioenergetics

Robert J. Usselman¹, Cristina Chavarriga², Pablo R. Castello³, Maria Procopio⁴, Thorsten Ritz⁴, Edward A. Dratz¹, David J. Singel¹ & Carlos F. Martino²

Received: 01 August 2016
Accepted: 10 November 2016
Published: 20 December 2016

Quantum biology is the study of quantum effects on biochemical mechanisms and biological function. We show that the biological production of reactive oxygen species (ROS) in live cells can be influenced by coherent electron spin dynamics, providing a new example of quantum biology in cellular regulation. ROS partitioning appears to be mediated during the activation of molecular oxygen (O_2) by reduced flavoenzymes, forming spin-correlated radical pairs (RPs). We find that oscillating magnetic fields at Zeeman resonance alter relative yields of cellular superoxide ($O_2^{\bullet-}$) and hydrogen peroxide (H_2O_2) ROS products, indicating coherent singlet-triplet mixing at the point of ROS formation. Furthermore, the orientation-dependence of magnetic stimulation, which leads to specific changes in ROS levels, increases either mitochondrial respiration and glycolysis rates. Our results reveal quantum effects in live cell cultures that bridge atomic and cellular levels by connecting ROS partitioning to cellular bioenergetics.

Quantum biology may be thought of as the signatures of molecular-level quantum phenomena observed in biological systems at functional, cellular, or organism levels^{1,2}. For example, quantum effects in biological systems have been implicated in mechanisms for avian navigation^{3–7}, olfactory sensing^{8,9}, and photosynthesis^{10–12}. Here, we present results that reveal a novel domain of quantum biology: the control of the biological production of reactive oxygen species (ROS) via coherent spin dynamics in a radical pair (RP) reaction. Our work builds on studies of complexes between reduced flavoenzymes and molecular oxygen^{13,14}, within the context of quantum biology¹⁵ and the radical pair mechanism (RPM)^{16,17}.

The RPM offers an attractive foundation to explain how quantum effects can influence biochemical ROS production. At the heart of the RPM lies a coherent singlet-triplet interconversion (Fig. 1), driven by the dynamical mixing of the spin eigenstates of coupled free-radicals. The RP spin dynamics are governed by internal magnetic interactions, usually electron-nuclear hyperfine interactions (HFIs) and applied magnetic fields. External static and oscillating magnetic fields can alter RP spin dynamics by Zeeman and HFI resonance effects, and thereby change the relative yields of reaction products that derive, alternatively, from singlet and triplet RP states^{18,19}. The product yields will depend on the strength of the static field and on the frequency, amplitude, and orientation (relative to the static field) of the applied oscillating magnetic field¹⁷. These experimental parameters can be adjusted to alter the relative ROS product yields *in vitro*. In this work, we demonstrate magnetic field-induced changes in ROS levels that leave a metabolic signature at the cellular level. We report the effects of the orientation of oscillating fields on the ROS reaction yields in cell cultures and the impact of the resulting variations in the ROS products on the regulation of cellular bioenergetics.

We assume that magnetically sensitive ROS formation occurs at flavoenzyme centers (Fig. 1), initialized by an electron transfer that activates molecular oxygen (O_2) in reduced flavoenzymes²⁰. A triplet-born, spin-correlated RP is created between flavin semiquinone ($FADH^{\bullet}$) and superoxide ($O_2^{\bullet-}$)^{21,22}. The $FADH^{\bullet}:O_2^{\bullet-}$ intermediate is a branch point for ROS products, where subsequent spin-selective reactions have two competing pathways. Either $O_2^{\bullet-}$ is released from the triplet RP state and escapes into the medium, or a hydroperoxy-flavin transient

¹Department of Chemistry and Biochemistry, Montana State University, Bozeman, MT 59717, USA. ²Department of Biomedical Engineering, Florida Institute of Technology, Melbourne, FL 32901, USA. ³Consejo Nacional de Investigaciones Científicas y Técnicas (CONICET), Universidad de Belgrano (UB), Villanueva 1324, C1426BMJ, Buenos Aires, Argentina. ⁴Department of Physics and Astronomy, University of California, Irvine, CA 92697, USA. Correspondence and requests for materials should be addressed to R.J.U. (email: robert.usselman@montana.edu) or C.F.M. (email: cmartino@fit.edu)

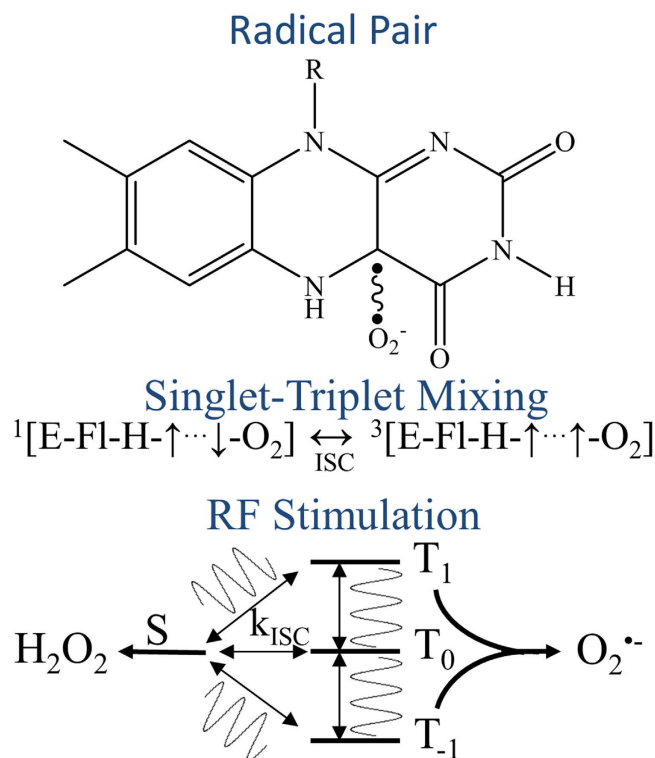


Figure 1. Flavin semiquinone (FADH[•]) and superoxide (O₂^{•-}) spin-correlated radical pair (top). The radical pair undergoes intersystem crossing (ISC) between singlet (S) and triplet states (T_{-1,0,1}) at rates (k_{ISC}) determined by electron-nuclear hyperfine and Zeeman interactions (middle). An applied RF oscillating magnetic field tuned at Zeeman resonance (1.4 MHz at 50 μ T magnetic field), modifies k_{ISC} (bottom), and ultimately affects the relative amount of singlet (H₂O₂) and triplet (O₂^{•-}) reaction products. Resonance effects on ROS product yields are a key manifestation of quantum biology.

is formed from the singlet RP state. A subsequent second electron transfer releases hydrogen peroxide (H₂O₂). Besides kinetic requirements²², the coherent evolution between the singlet and triplet states of FADH[•]:O₂^{•-} RP determines the amount of the products for the two reaction channels. We hypothesize that RP spin dynamics can be altered by external static and oscillating magnetic fields²³, which change singlet-triplet intersystem crossing (ISC) rates, and thus affect the outcome of cellular ROS product ratios.

To test the RPM hypothesis for ROS-related quantum biology, we developed low-frequency, low-field instrumentation for product-yield detected magnetic resonance (PYDMR)²¹. In the present PYDMR study, primary human umbilical vein endothelial cells (HUVECs) were exposed to either 50 μ T static magnetic fields (SMF) in control samples, or to 50 μ T SMFs combined with 1.4 MHz, 20 μ T_{rms} RF magnetic fields at Zeeman resonance in experimental samples. The RF orientation was applied in parallel or perpendicular angles with respect to the SMF. Intracellular O₂^{•-} and extracellular H₂O₂ were measured by selective assays in HUVEC cultures. Figure 2 exhibits the changes observed in the ROS product distributions measured for parallel and perpendicular RF orientations. In the perpendicular orientation, we measured a 36% \pm 4 reduction of O₂^{•-} ($p < 0.002$) and a 21% \pm 5 reduction of H₂O₂ ($p < 0.02$). For the parallel orientation, we measured a 10% \pm 2 ($p < 0.002$) reduction of O₂^{•-} and an 8% \pm 8 increase of H₂O₂ ($p < 0.02$). Changes in ROS products in cell cultures between SMF \pm RF are indicative of a resonance effect on singlet-triplet intersystem crossing (or quantum coherences) at the point of ROS formation²¹.

Singlet-triplet product yields were modeled by numerical simulations of a triplet-born one-proton radical-pair reaction with static and RF magnetic fields at Zeeman resonance⁷, Fig. 3. The numerical results predict an orientation-dependent increase in singlet product yield (H₂O₂) and decrease in triplet product yield (O₂^{•-}) when the resonant RF field is added to the static field. These simulations are in agreement with perpendicular experimental results (Fig. 2) and are consistent with our previous cellular results with hyperfine resonance effects²¹. The theoretical model of a one-proton RP does not account for changes in ROS yields (O₂^{•-} and H₂O₂) in the parallel orientation, which suggests either limitations of the simplified model in the complex cellular environment or anisotropic hyperfine resonances near the Zeeman resonance.

To understand the potential effects of ROS signaling on cellular bioenergetics, we measured the oxygen consumption rate (OCR) and extracellular acidification rate (ECAR) with a Seahorse XF Analyzer, Fig. 4. OCR indicates the mitochondrial respiration rate and ECAR is predominately a measure of lactic acid formed during glycolytic energy metabolism^{24,25}. Figure 4 illustrates experiments in HUVECs that show RF orientation dependence of OCR and ECAR bioenergetic measurements, which appear to result from changes in ROS partitioning. Zeeman resonance at perpendicular excitation did not affect OCR levels (Fig. 4A) but increased ECAR by

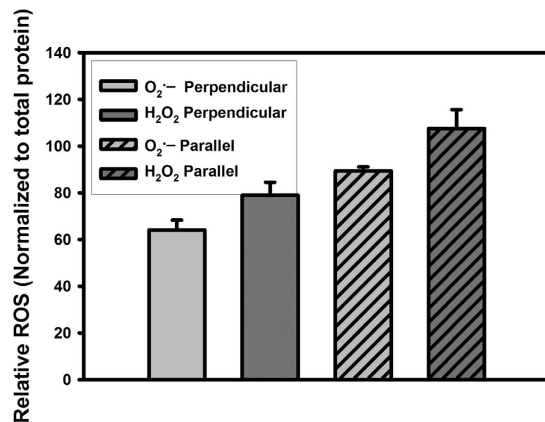


Figure 2. ROS product distributions illustrating the RF magnetic field orientation dependence at Zeeman resonance (1.4 MHz and 50 μ T magnetic field). The data is presented as a product yield ratio percentage with \pm RF in the static field. RF magnetic fields in perpendicular orientation decreased both O₂⁻ and H₂O₂ levels by 36% \pm 4% ($p < 0.002$) and 21% \pm 5% ($p < 0.02$), respectively, relative to controls. In parallel orientation, H₂O₂ levels increased by 8% \pm 8% ($p < 0.02$), whereas O₂⁻ decreased by 10% \pm 2% ($p < 0.002$), relative to controls. The amount of ROS produced were normalized to protein concentrations and represent the average of 3 independent experiments.

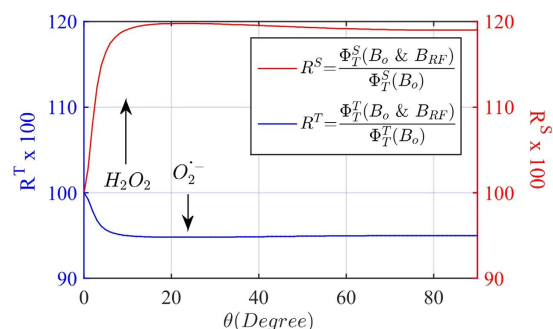


Figure 3. Numerical simulations of the effects of RF magnetic fields at Zeeman resonance on triplet (Φ_T^T , O₂⁻) and singlet (Φ_T^S , H₂O₂) yields of a triplet-born radical-pair reaction. The RP model shown here is for a one-proton radical-pair with one isotropic hyperfine coupling of 500 μ T and a RP lifetime of 10 μ s. The static magnetic field was set to B₀ = 50 μ T and the RF magnetic field amplitude set to B_{RF} = 20 μ T (RMS), with a Zeeman resonance frequency of 1.4 MHz. R^T (R^S) is the relative change of triplet (singlet) yields produced by the RF, relative to the levels in the static field.

100% \pm 13 (Fig. 4C). Zeeman resonance at parallel excitation had an opposite effect, where OCR increased by 54% \pm 4 (Fig. 4B) while ECAR remained unchanged (Fig. 4D). Altered OCR and ECAR values indicate phenotypic changes in HUVECs bioenergetic pathways, demonstrating spin biochemistry intervention of ROS signaling by RF magnetic fields at Zeeman resonance.

The orientation effects that lead to specific ROS product distributions are in agreement with the simple RPM model for the perpendicular orientation, which predicts an increase in singlet yields with a concomitant decrease in triplet yields, Fig. 3. The overall reduction in measured ROS products at perpendicular excitation suggests a possible ROS signaling link to increased glycolytic activity^{26,27}. The decrease in steady-state ROS levels with enhanced glycolytic activity might be due to scavenging of ROS by pyruvate²⁸. The differential effect on ROS product yields at parallel excitation indicate a signaling channel of increased mitochondrial respiration. Our experiments did not explore the downstream targets of the ROS signaling pathways that lead to regulation of glycolysis and respiration. We suggest that ROS signaling channels are likely to involve the activation of bioenergetic regulation proteins^{26,29,30}, eliciting a type of hormesis response³¹ or a Warburg effect²⁷.

Magnetic stimulation of ROS partitioning in live cells reveals hallmarks of quantum coherence, manifested by changes in cellular ROS product distributions. Changes in ROS product partitioning, in turn, altered cellular bioenergetics by increasing either mitochondrial respiration or glycolysis. ROS formation is inextricably linked to bioenergetics by normal cellular metabolism, connecting persistent quantum effects in ROS oxidative signaling to cellular bioenergetics. Because of the importance of ROS in human health and disease³², this research is likely to have significance for several areas in bio-medical research. Our results provide fundamental insights into the role of the RPM in ROS redox biology and cellular bioenergetics, revealing a new example of quantum biology.

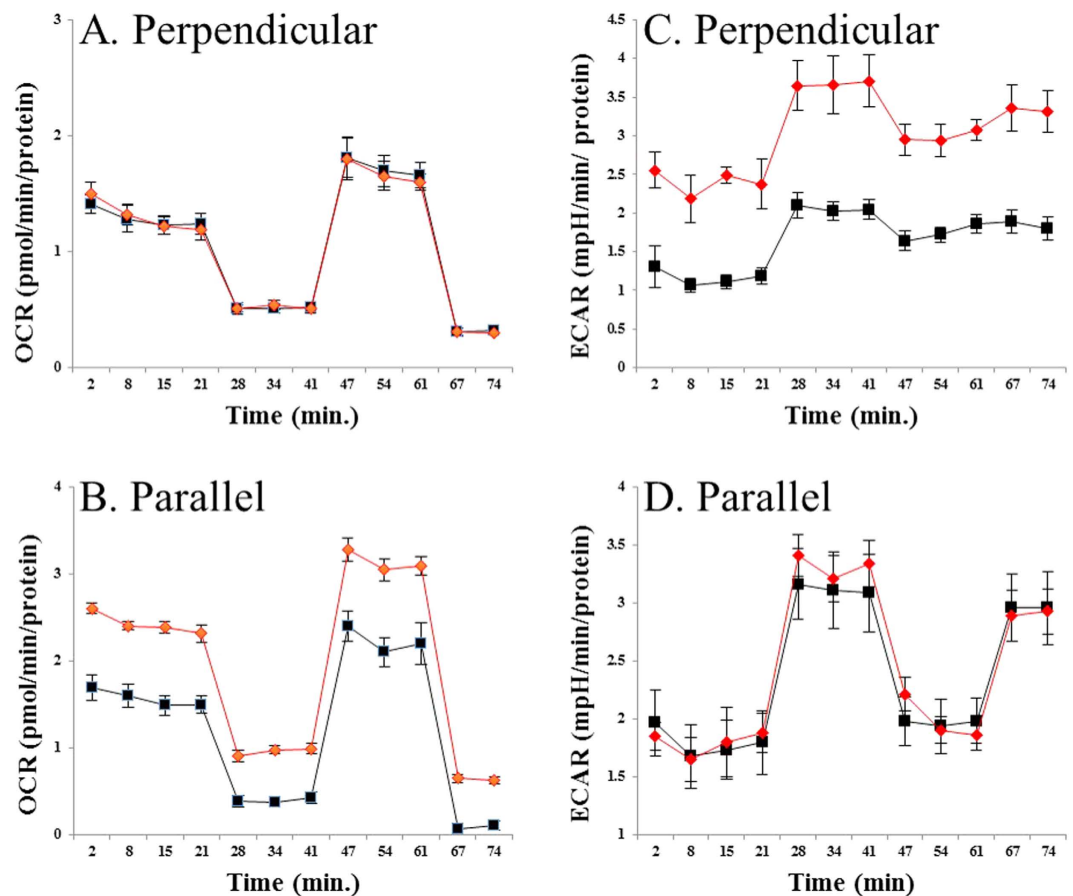


Figure 4. Bioenergetic profiles of HUVECs cultures monitored with a Seahorse XF Analyzer, comparing static alone (■) and static + RF (♦) magnetic fields. Oligomycin was added at 21 min to inhibit ATP synthesis, the proton ionophore FCCP was added at 41 min to assess the maximum possible oxygen consumption, and antimycin A was added at 61 min to inhibit electron flow through complex III. The static magnetic field was $50\ \mu\text{T}$ and the RF was 1.4 MHz at Zeeman resonance. The RF was oriented perpendicular (A and C) or parallel (B and D) to the static field. Perpendicular RF excitation did not affect the oxygen consumption rate (OCR) (Panel A), whereas extracellular acidification rate (ECAR) was increased by 100 ± 13 ($p < 0.001$, Panel C). Parallel RF excitation lead to increased OCR by 54 ± 4 ($p < 0.001$, Panel B), while ECAR remained unchanged (Panel D). These are results of 3 independent representative experiments and data were normalized to total cellular protein.

Methods

Cell Culture. Human umbilical vein endothelial cells (HUVECs) (passage 2–4) were cultured in endothelial growth medium (Promocell GmbH, Heidelberg, Germany) supplemented with 2% fetal calf serum (FCS), 0.004 ml/ml endothelial cell growth supplement/heparin, 0.1 ng/ml epidermal growth factor (EGF), 1 ng/ml basic fibroblast growth factor, and 1 mg/ml hydrocortisone at 37°C with 5% CO_2 . The cells were cultured in a 75- cm^2 flask to expand cell number. After reaching confluence, the cells were seeded in (a) 6-well culture plates at a density of 3.5×10^3 cells/ cm^2 for ROS experiments; (b) and in mini plates at 3,500 cells per well for Seahorse XFp Analyzer (Agilent Technologies, Santa Clara, CA).

ROS Measurements. Cellular H_2O_2 production was measured with the horseradish peroxidase-linked Amplex Ultra Red (HRP-AUR) fluorometric assay (Invitrogen). After cells were seeded, they were exposed to SMF \pm RF magnetic fields for the duration of the experiment, by use of the PYDMR apparatus we previously described²¹. At day 3, medium was aspirated and cells were washed with Hank's Buffer (HB) with $100\ \mu\text{M}$ diethylenetriaminepentaacetic acid (DTPA) and incubated for 1 h with HB containing $10\ \mu\text{M}$ AUR and 0.2 units/ml HRP. Resorufin fluorescence was collected on a Gemini fluorescence microplate reader (Molecular Devices, Sunnyvale, CA).

To measure intracellular production of $\text{O}_2^{\bullet-}$, HUVECs were incubated for 30 min at 37°C in HB containing $50\ \mu\text{M}$ dihydroethidium (DHE) at day 3. Cells were washed twice in HB with $100\ \mu\text{M}$ DTPA and harvested in 300 μL of methanol. The samples were spun down for 15 min at 12,000 rpm at 4°C , the supernatant was collected and dried for 5–6 hrs at 37°C and stored at -20°C for 7–10 days before high-performance liquid chromatography (HPLC) analysis. An Agilent 1100 series HPLC with a G1321A fluorescence detector was used for DHE product

separation. Analytes were separated using a C-18 reverse-phase column (Nucleosil 250 to 4.5 mm) as previously described³³. The total fluorescence intensity of the 2-hydroxyethidium peak were averaged for all wells and then averaged for three separate experiments.

Protein content, HPLC analysis, and resorufin fluorescence were measured at the same termination points. H₂O₂ and O₂^{•-} measurements were normalized to total protein concentration (BCA, Pierce). H₂O₂ calibration curves with HRP-AUR under the same RF magnetic field strengths showed no differences compared to SMF controls, demonstrating that RF fields do not interact with the H₂O₂ detection assay.

Cellular Bioenergetics. An XFp Analyzer from Seahorse Bioscience was used for the bioenergetic measurements. HUVECs were seeded at 4,000 cells per well in XFp miniplates and exposed to RF magnetic fields for 2 days. The MitoStress Test Assay was performed as described previously^{24,25}. The XFp Analyzer measured mitochondrial respiration and glycolysis *in vitro*^{34,35} in the same samples. Mitochondrial respiration was determined by the oxygen consumption rate (OCR) in cell culture. Glycolysis was assessed by the extracellular acidification rate (ECAR). To estimate the proportion of the OCR coupled to ATP synthesis, oligomycin (1 µg/ml) was injected at 21 minutes into all samples to inhibit the ATP synthase. Typically, the OCR rate decreases in response to oligomycin by the extent to which the cells are using mitochondria to generate ATP. The remaining OCR can be ascribed to both proton leak across the mitochondrial membrane and oxygen consumption by processes other than reduction at cytochrome c oxidase. To determine the maximal OCR that the cells can sustain, the proton ionophore (uncoupler) FCCP (1 µM) was injected at 41 minutes. Lastly, antimycin A (10 µM) is injected at 61 minutes to inhibit electron flux through Complex III, which suppresses OCR dramatically. What remains is the OCR that is attributable to O₂ consumption due to the formation of mitochondrial ROS and non-mitochondrial sources.

References

- Ball, P. Physics of life: The dawn of quantum biology. *Nature* **474**, 272–274, doi: 10.1038/474272a (2011).
- Lambert, N. *et al.* Quantum Biology. *Nature Physics* **9**, 10–18 (2013).
- Maeda, K. *et al.* Chemical compass model of avian magnetoreception. *Nature* **453**, 387–U338, doi: 10.1038/nature06834 (2008).
- Ritz, T., Adem, S. & Schulten, K. A model for photoreceptor-based magnetoreception in birds. *Biophys J* **78**, 707–718 (2000).
- Gegebar, R. J., Foley, L. E., Casselman, A. & Reppert, S. M. Animal cryptochromes mediate magnetoreception by an unconventional photochemical mechanism. *Nature* **463**, 804–807, doi: 10.1038/nature08719 (2010).
- Solov'yov, I. A. & Schulten, K. Magnetoreception through Cryptochrome May Involve Superoxide. *Biophys J* **96**, 4804–4813, doi: 10.1016/j.bpj.2009.03.048 (2009).
- Ritz, T., Thalau, P., Phillips, J. B., Wiltschko, R. & Wiltschko, W. Resonance effects indicate a radical-pair mechanism for avian magnetic compass. *Nature* **429**, 177–180, doi: 10.1038/nature02534 (2004).
- Turin, L. A spectroscopic mechanism for primary olfactory reception. *Chem Senses* **21**, 773–791, doi: 10.1093/chemse/21.6.773 (1996).
- Turin, L., Skoulakis, E. M. C. & Horsfield, A. P. Electron spin changes during general anesthesia in *Drosophila*. *P Natl Acad Sci USA* **111**, E3524–E3533, doi: 10.1073/pnas.1404387111 (2014).
- Engel, G. S. *et al.* Evidence for wavelike energy transfer through quantum coherence in photosynthetic systems. *Nature* **446**, 782–786, doi: 10.1038/nature05678 (2007).
- Lee, H., Cheng, Y. C. & Fleming, G. R. Coherence dynamics in photosynthesis: Protein protection of excitonic coherence. *Science* **316**, 1462–1465, doi: 10.1126/science.1142188 (2007).
- Marais, A., Sinayskiy, I., Petruccione, F. & van Grondelle, R. A quantum protective mechanism in photosynthesis. *Sci Rep-Uk* **5**, doi: 10.1038/srep08720 (2015).
- Bruice, T. C. Oxygen-Flavin Chemistry. *Israel Journal of Chemistry* **24**, 54–61, doi: 10.1002/ijch.198400008 (1984).
- Massey, V. Activation of Molecular-Oxygen by Flavins and Flavoproteins. *J Biol Chem* **269**, 22459–22462 (1994).
- Mohseni, M. O. Y., Engel, G. S. & Plenio, M. B. *Quantum Effects in Biology*. (Cambridge University Press, 2014).
- Grissom, C. B. Magnetic-Field Effects in Biology - a Survey of Possible Mechanisms with Emphasis on Radical-Pair Recombination. *Chemical Reviews* **95**, 3–24, doi: 10.1021/cr00033a001 (1995).
- Steiner, U. & Ulrich, T. Magnetic field effects in chemical kinetics and related phenomena. *Chemical Reviews* (1989).
- Canfield, J. M., Belford, R. L., Debrunner, P. G. & Schulten, K. J. A Perturbation-Theory Treatment of Oscillating Magnetic-Fields in the Radical Pair Mechanism. *Chem Phys* **182**, 1–18, doi: 10.1016/0301-0104(93)E0442-X (1994).
- Schulten, K., Staerk, H., Weller, A., Werner, H. J. & Nickel, B. Magnetic-Field Dependence of Geminate Recombination of Radical Ion-Pairs in Polar-Solvents. *Z Phys Chem Neue Fol* **101**, 371–390 (1976).
- Imlay, J. A. The molecular mechanisms and physiological consequences of oxidative stress: lessons from a model bacterium. *Nature reviews. Microbiology* **11**, 443–454, doi: 10.1038/nrmicro3032 (2013).
- Usselman, R., Hill, I., Singel, D. & Martino, C. Spin Biochemistry Modulates Reactive Oxygen Species (ROS) Production by Radio Frequency Magnetic Fields *PLoS ONE* **9**, e93065, doi: 10.1371/journal.pone.0093065 (2014).
- Hogben, H. J., Efimova, O., Wagner-Rundell, N., Timmel, C. R. & Hore, P. J. Possible involvement of superoxide and dioxygen with cryptochrome in avian magnetoreception: Origin of Zeeman resonances observed by *in vivo* EPR spectroscopy. *Chem Phys Lett* **480**, 118–122, doi: 10.1016/j.cplett.2009.08.051 (2009).
- Timmel, C. R., Till, U., Brocklehurst, B., McLauchlan, K. A. & Hore, P. J. Effects of weak magnetic fields on free radical recombination reactions. *Mol Phys* **95**, 71–89, doi: 10.1080/00268979809483134 (1998).
- Dranka, B. P. *et al.* Assessing bioenergetic function in response to oxidative stress by metabolic profiling. *Free radical biology & medicine* **51**, 1621–1635, doi: 10.1016/j.freeradbiomed.2011.08.005 (2011).
- Dranka, B. P., Hill, B. G. & Darley-Usmar, V. M. Mitochondrial reserve capacity in endothelial cells: the impact of nitric oxide and reactive oxygen species. *Free radical biology & medicine* **48**, 905–914, doi: 10.1016/j.freeradbiomed.2010.01.015 (2010).
- Liemburg-Apers, D. C., Willems, P. H. G. M., Koopman, W. J. H. & Grefte, S. Interactions between mitochondrial reactive oxygen species and cellular glucose metabolism. *Arch Toxicol* **89**, 1209–1226, doi: 10.1007/s00204-015-1520-y (2015).
- Vander Heiden, M. G., Cantley, L. C. & Thompson, C. B. Understanding the Warburg effect: the metabolic requirements of cell proliferation. *Science* **324**, 1029–1033, doi: 10.1126/science.1160809 (2009).
- Brand, K. A. & Hermfisse, U. Aerobic glycolysis by proliferating cells: a protective strategy against reactive oxygen species. *The FASEB Journal* **11**, 388–395 (1997).
- Mailloux, R. J. & Harper, M. E. Uncoupling proteins and the control of mitochondrial reactive oxygen species production. *Free Radical Bio Med* **51**, 1106–1115, doi: 10.1016/j.freeradbiomed.2011.06.022 (2011).

30. Willems, P. H. G. M., Rossignol, R., Dieteren, C. E. J., Murphy, M. P. & Koopman, W. J. H. Redox Homeostasis and Mitochondrial Dynamics. *Cell Metab* **22**, 207–218, doi: 10.1016/j.cmet.2015.06.006 (2015).
31. Ji, L. L., Kang, C. & Zhang, Y. Exercise-induced hormesis and skeletal muscle health. *Free Radic Biol Med*, doi: 10.1016/j.freeradbiomed.2016.02.025 (2016).
32. Brieger, K., Schiavone, S., Miller, F. J. & Krause, K. H. Reactive oxygen species: from health to disease. *Swiss Med Wkly* **142**, doi: 10.4414/smww.2012.13659 (2012).
33. Fink, B. *et al.* Detection of intracellular superoxide formation in endothelial cells and intact tissues using dihydroethidium and an HPLC-based assay. *Am J Physiol Cell Physiol* **287**, C895–902, doi: 10.1152/ajpcell.00028.2004 (2004).
34. Gerencser, A. A. *et al.* Quantitative Microplate-Based Respirometry with Correction for Oxygen Diffusion. *Analytical Chemistry* **81**, 6868–6878, doi: 10.1021/ac900881z (2009).
35. Wu, M. *et al.* Multiparameter metabolic analysis reveals a close link between attenuated mitochondrial bioenergetic function and enhanced glycolysis dependency in human tumor cells. *Am J Physiol-Cell Ph* **292**, C125–C136, doi: 10.1152/ajpcell.00247.2006 (2007).

Acknowledgements

This work was supported by American Heart Association Grant #15SDG25710461 (R.J.U.), and PIP 706 Consejo Nacional de Investigaciones Científicas y Técnicas (CONICET) (P.R.C).

Author Contributions

R.J.U., P.R.C. and C.F.M. designed the experiments, C.C., R.J.U. and C.F.M performed the experiments, M.P., performed the spin dynamics simulations, M.P., T.R. and D.J.S contributed to theoretical aspects of the RPM, P.R.C. and E.A.D. contributed to bioenergetics. R.J.U. wrote the initial paper draft and all authors contributed to manuscript revisions.

Additional Information

Competing financial interests: The authors declare no competing financial interests.

How to cite this article: Usselman, R. J. *et al.* The Quantum Biology of Reactive Oxygen Species Partitioning Impacts Cellular Bioenergetics. *Sci. Rep.* **6**, 38543; doi: 10.1038/srep38543 (2016).

Publisher's note: Springer Nature remains neutral with regard to jurisdictional claims in published maps and institutional affiliations.



This work is licensed under a Creative Commons Attribution 4.0 International License. The images or other third party material in this article are included in the article's Creative Commons license, unless indicated otherwise in the credit line; if the material is not included under the Creative Commons license, users will need to obtain permission from the license holder to reproduce the material. To view a copy of this license, visit <http://creativecommons.org/licenses/by/4.0/>

© The Author(s) 2016